

Hyperspectral Imaging of Rivers and Estuaries

Curtiss O. Davis* and Nicholas Tufillaro

College of Earth, Ocean and Atmospheric Sciences, Oregon State University, 104 CEOAS Admin. Bldg., Corvallis, OR USA 97331-5503

ABSTRACT

The Hyperspectral Imager for the Coastal Ocean (HICO) is the first spaceborne imaging spectrometer designed to sample the coastal ocean. HICO samples selected coastal regions at 92 m ground sample distance with full spectral coverage (88 channels covering 400 to 900 nm) and a high signal-to-noise ratio to resolve the complexity of the coastal ocean. HICO has been operating on the International Space Station since October 2009 and collected over 8000 scenes for more than 50 users. We have been using HICO data to study major rivers and estuaries in the US and Asia. Our results show the advantages of HICO's additional spectral channels and higher spatial resolution for studying these complex coastal waters. We use these data to suggest requirements for spatial and spectral sampling for future ocean color sensors.

Keywords: Hyperspectral imaging, coastal ocean, rivers, estuaries

1. INTRODUCTION

The coastal ocean is a rich and complex environment. Over half of humanity lives on the coast or along river systems, utilizing water resources for transportation, waste disposal, fisheries, and industries such as oil and gas production. At the same time it is a difficult environment for visible remote sensing; ocean scenes are dark relative to land scenes because of water absorption, and coastal scenes are often spatially and spectrally complex due a wide assortment of sediments from land runoff, as well as pigments from biological productivity, such as plankton blooms. All of these color agents are mixed together by tidal forcing and strong coastal currents. To unravel this complexity the Hyperspectral Imager for the Coastal Ocean (HICO) was designed as the first spaceborne imaging spectrometer to specifically sample the coastal ocean. HICO targets selected coastal regions at 92 m ground sample distance with full spectral coverage (88 channels between 400 to 900 nm), and a high signal-to-noise ratio to resolve the complexity of the coastal ocean^{1,2}. The on-orbit radiometric calibration of HICO is maintained using ground reference sites and the spectral calibration is maintained using the atmospheric and solar absorption lines³.

HICO has been operating on the International Space Station since October 2009 and to date has captured over 8000 images for more than 50 users. Further information about HICO, current HICO projects and access to the data is available through the Oregon State University HICO website (<http://hico.coas.oregonstate.edu>). The initial Office of Naval Research funded HICO mission was completed in December 2012. Since January 1, 2013 HICO operations have been supported by the NASA International Space Station Science Program. NASA operations include the distribution of HICO data through the NASA Ocean Color Website (<http://oceancolor.gsfc.nasa.gov>). We have been using HICO data to study rivers and estuaries in the U.S. and Asia. HICO's higher spatial resolution and continuous spectral sampling have proven extremely valuable for the studies reported here.

2. SPECTRAL ANALYSIS METHODS

A key advantage of HICO is the continuous spectra for each pixel; this opens up the opportunity for new water remote sensing algorithms that go beyond band ratios, and build upon analytic spectroscopy techniques developed in laboratories over decades. One example is derivative analysis; derivatives highlight abrupt changes in spectral shape indicating absorption and scattering features. Using derivative analysis we can assess the best wavelengths needed to sample various features, such as bottom sediments, river plumes or algal blooms^{4,5,6}. In effect, derivative analysis is just one of many methods that attempt to reduce the dimension of a hyperspectral data set to focus it on specific biogeochemical water constituents. Other approaches include the reduction of the dimension of hyperspectral data sets by linear methods such as principle components^{7,8}, or nonlinear methods such as manifold learning⁹.

*cdavis@coas.oregonstate.edu; Phone: 541-737-5707; Fax: 541-737-2064

2.1 Derivative Analysis

The use of derivative analysis for spectroscopic data is a standard technique in laboratory analysis, and we adapt those techniques for use with data from HICO^{10,11}. In particular, the derivative is computed with a Savitzky-Golay (S-G) smoothing and differentiation filter¹². The nominal HICO data spectral resolution is 5.7 nm, and using the S-G filter the spectral data is interpolated to a 2 nm grid, with a 3rd order polynomial and a window length of 9 nm.

Oddly, in order to *reduce* the dimension of a hyperspectral data set, we first *increase* the dimension by estimating derivatives of the spectra (the slope) with respect to wavelength. The reason is illustrated in Fig. 1, which shows the spectra taken from a transect across the Elwha River plume. As the transect crosses the river plume, the (negative) slope of the spectra shows a rapid change between 700 – 730 nm, presumably due to a combination of bright backscatter from sediments and strong absorption by water in this spectral region. An estimate of the slope from the first derivative centered at 716 nm is sensitive to the signal from the river plume, and relatively insensitive to other constituents in the water or atmosphere.

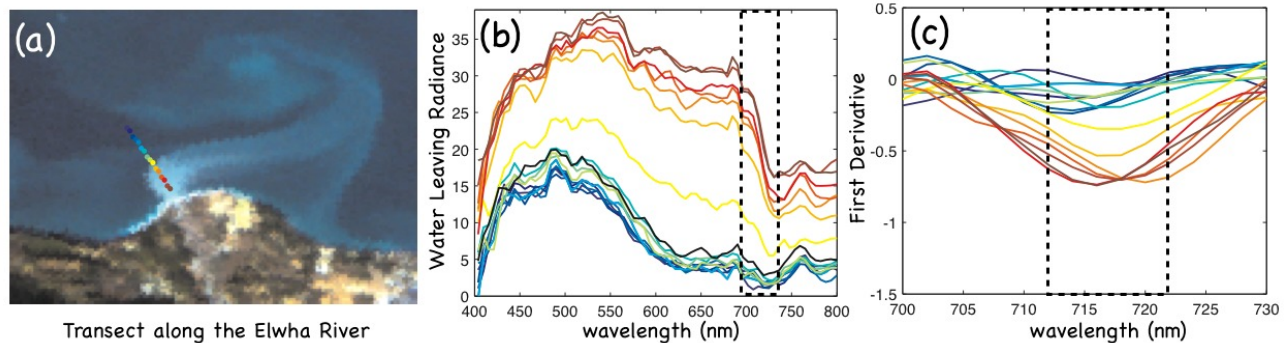


Figure 1. HICO image and derivative spectra from a transect crossing the Elwha River plume in Washington State, USA (10 January 2012). (a) Image (note the transect crossing the river plume indicated by the dots from blue to red). (b) Spectra corresponding to transect. (c) First derivative of spectra centered about 716 nm along transect where the spectra in (b) show a rapid change in slope as they cross the river plume.

2.2 Phase Difference Function

When spectra are described by continuous signals parameterized by wavelength, it is possible to study the intrinsic geometry of the data. Using hyperspectral data and its derivatives, we defined a phase difference function that can be valuable in detecting rapid changes in the intrinsic geometry of spectra. Computing the first and second derivative defines a 3-dimensional geometry for a spectrum, $(x, y, z) = (s, s', s'') = \mathbf{z}(\lambda)$, where $s(\lambda)$ is the spectrum of interest, and s' , s'' denote its first and second derivative with respect to the wavelength, λ . The vector $\mathbf{z}(\lambda)$ defines a natural phase angle, and rapid changes of the phase of $\mathbf{z}(\lambda)$ over a spatial transect, centered on narrow spectral bands, can be used to detect fronts and interfaces as we illustrate below. More details of the method are described in¹³.

3. RIVER SYSTEMS

3.1 Elwha River, Washington, USA

The Elwha River is being returned to its natural state. The largest dam-removal project in history began in September 2011 on the Elwha River of Washington State. The project, which aims to restore the river ecosystem and increase imperiled salmon populations that once thrived there, provides a unique opportunity to better understand the implications of large-scale river restoration¹⁴. One of the consequences was the release of more than 19 million cubic meters of sediment stored in both reservoirs into the downstream system. We have been monitoring the sediment plume entering the Straits of Juan de Fuca at the Elwha River mouth to look at the redistribution of those sediments. Figure 1 is an example of the visible sediment plume and the use of derivative products to map that plume.

3.2 Yangtze River, China

The Yangtze (Changjiang) River, the largest river in China and fifth largest in the world, provides a dramatic example of sediment and nutrient transport. The Yangtze River inputs a large amount of nutrients and sediments into the East China Sea (ECS) which is home to one of the largest and most productive fisheries in the world. Construction and filling of

Three Gorges Dam is dramatically reducing the water flow and nutrient input to the ECS affecting this important fishery¹⁵. The Yangtze carries a large sediment load¹⁶ and the coastal waters are highly reflective as shown in Figure 2.

Figure 2 shows a sequence of clear HICO images of the Yangtze River in China along with typical plots of the second derivative of the spectrum with respect to wavelength. The wavelengths around 620 nm are sensitive to sediment concentrations, and MERIS¹⁷ uses a 620 nm channel to estimate sediment. As also pointed out by¹⁸, who studied phytoplankton pigments using HICO, hyperspectral images allow us to optimize the wavelengths used in product algorithms for specific regions. In the Yangtze River region, for example, the maximum sensitivity to sediment concentration occurs at 605 nm rather than 620 nm. Our principal component method, like optimized band ratio methods¹⁸ will weight the sediment product algorithm with an optimized sediment maximum that is trained on regional data (Fig. 3).

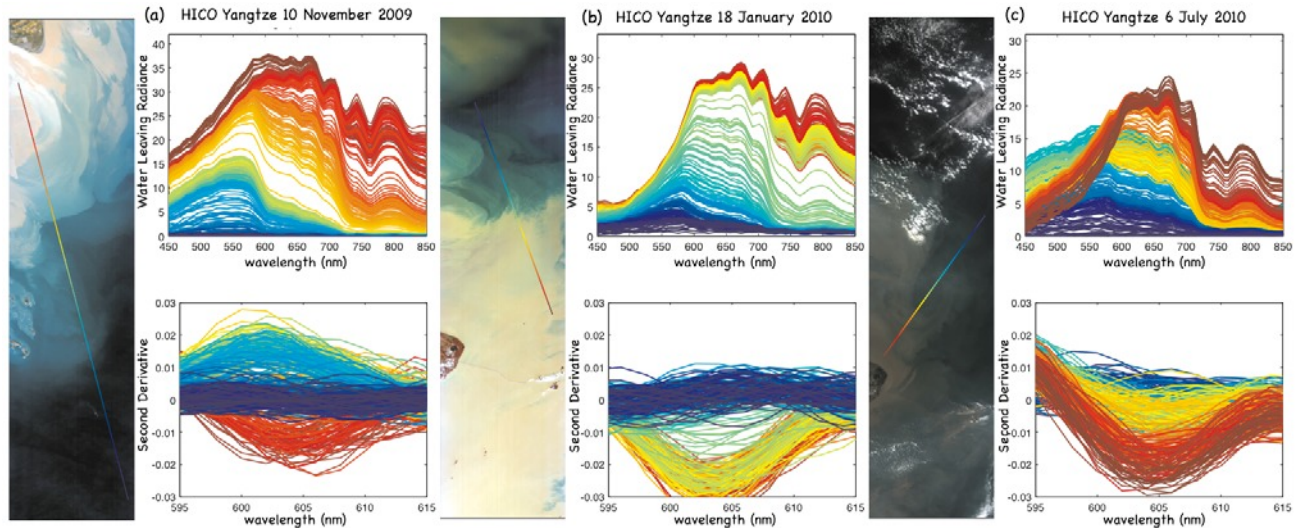


Figure 2. HICO images and derivative spectra of the Yangtze River in China. Using collections of images we are building up signatures to distinguish the constituents of the water column for this region. This sequence of images and spectra illustrates a consistent (negative) extrema for Yangtze River sediments in the second derivative around 605 nm. The spectra are taken from the rainbow-colored transect indicated in each image.

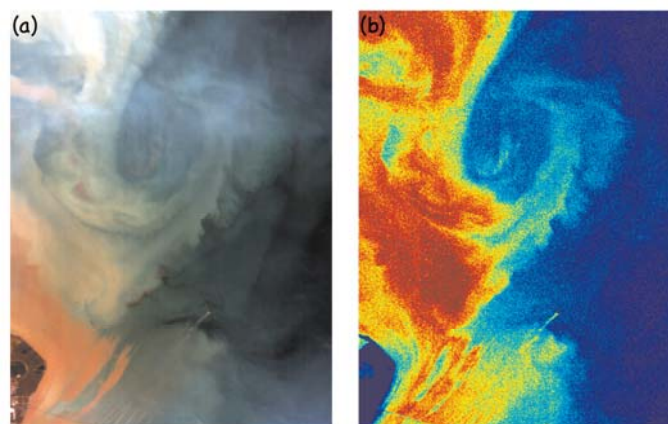


Figure 3. (a) HICO RGB image and (b) sediment product map for Yangtze River, China on 6 July 2010. Fig. 2 (c) shows the second derivative of the spectrum around 605 nm, which is more sensitive to sediment concentration than the 620 nm MERIS band 6. Our HICO product algorithm automatically optimizes the product algorithm to weight data more heavily around 605 nm when trained on Yangtze regional historical data, like those presented in Fig. 2.

3.3 Columbia River, USA

The Columbia River is the largest river in the Western United States collecting water from 5 states and British Columbia, Canada. The Columbia River plume is one of the dominant features of the California Current System and it plays a key role in the physical and biogeochemical functioning of that system off the Oregon and Washington coasts. The traditional picture of the Columbia plume is that it is oriented southwest offshore the Oregon coast in summer and north along the Washington coast in winter. Recent studies by Hickey et al.¹⁹ have shown that it is more complex and typically bi-directional in the summer with branches both north and south with the features moving in response to changing wind stress. The physics is now well known and the complex plume dynamics have been modeled in detail²⁰. Tides, river flow, wind forcing and large scale circulation patterns all play a role controlling the size and location of the plume.

Derivative analysis can be combined with the method of principle components to build regionally tuned maps of sediment concentration. Using methods similar to those described by Ortiz, we computed the principle components based on the first-derivative of HICO data along the mouth of the Columbia River^{7,8}. Computing the first derivative of sediment rich waters from the Columbia River indicated a correlation weighted around 590 nm (Fig 4). Example sediment maps using principle components are shown in Fig. 5. Since the maps are weighted toward the sediment-laden background waters, they naturally highlight objects with different reflectance on this background, such as boats as shown in Fig. 6.

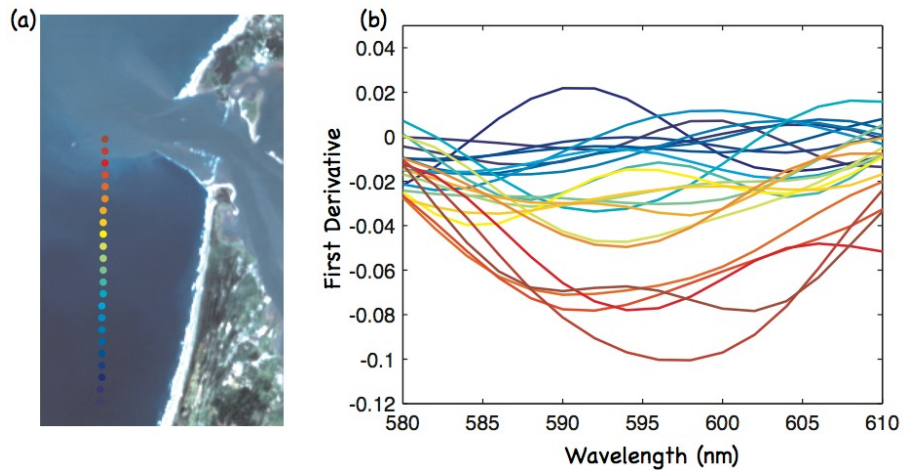


Figure 4. (a) HICO and transect taken for spectrum of the Columbia River Mouth on 12 May 2012. (b) The first derivative of the spectrum shows (negative) extrema around 595 nm for sediment-laden waters.

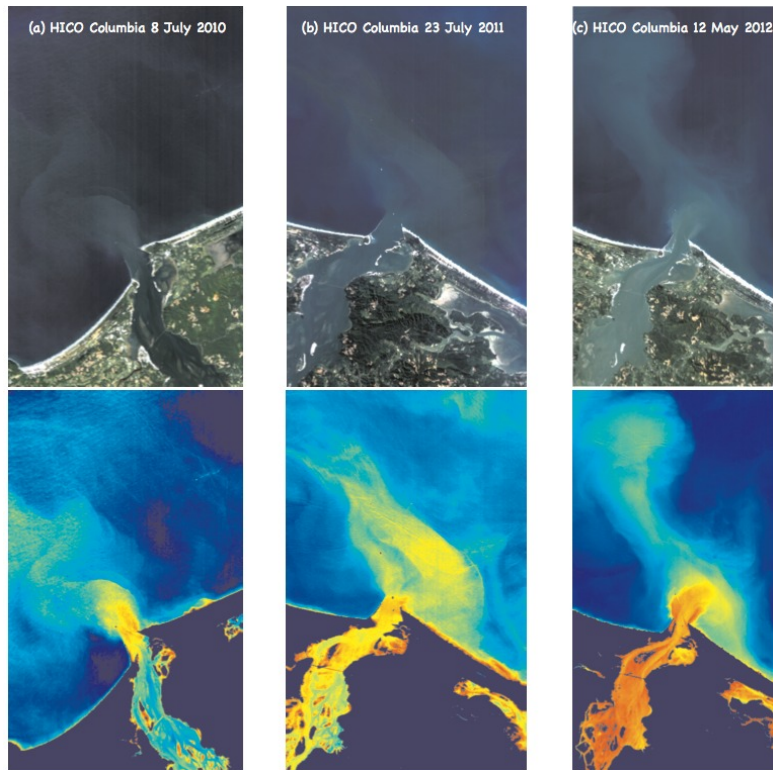


Figure 5. HICO images of the Columbia River Mouth. The top images show RGB for the indicated dates. The bottom images are sediment maps based on a principle components decomposition of the hyperspectral basis functions.

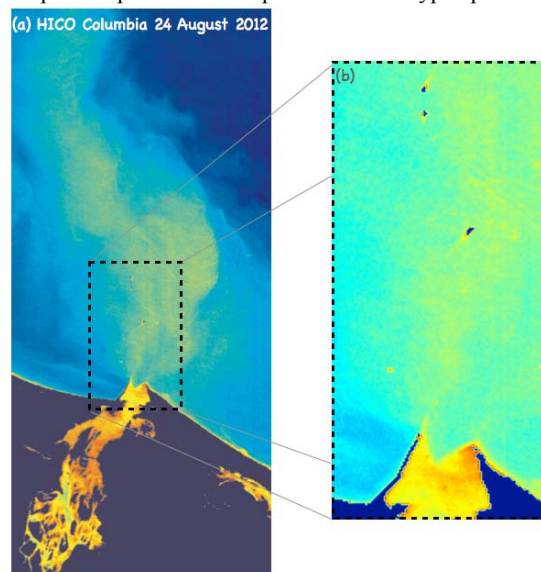


Figure 6. Sediment map of the Columbia River Mouth based on principle components decomposition. Since boats have a different spectral signature (different weighting of principle component basis functions) they are easily differentiated from the background sediment rich water.

3.4 San Francisco Bay, USA

The Sacramento and San Joaquin rivers and tributaries drain most of California and flow into the San Francisco Bay. This collective system has important interplay with human population and economics, especially in regions of high

population density like the San Francisco Bay and Delta Ecosystem (SFE). The SFE is the largest estuary on the Pacific coast of the United States and the largest wetland habitat in the western U.S. It is a critical ecosystem that links freshwater and marine environments providing essential habitat for fish, drinking water to over 22 million urban users, and irrigation water for agriculture in the highly productive Central Valley. HICO imagery provides a fresh insight into this complex system and here we examine the water exiting the bay.

Fig. 7 shows an example of a phase difference function for water masses that appear inside and outside of the edge of what appears to be the bay water and sea water mixing interface. The red pixels in Fig. 7c highlight areas that contain a jump in the phase difference centered at 709 nm, revealing patches of presumably high algal concentrations that exist at the interface of the bay and sea waters. This bloom could be a result of large amounts of nutrients, particularly ammonia from sewage plants, that are released in the Sacramento River and San Francisco Bay system but not utilized in the Bay.

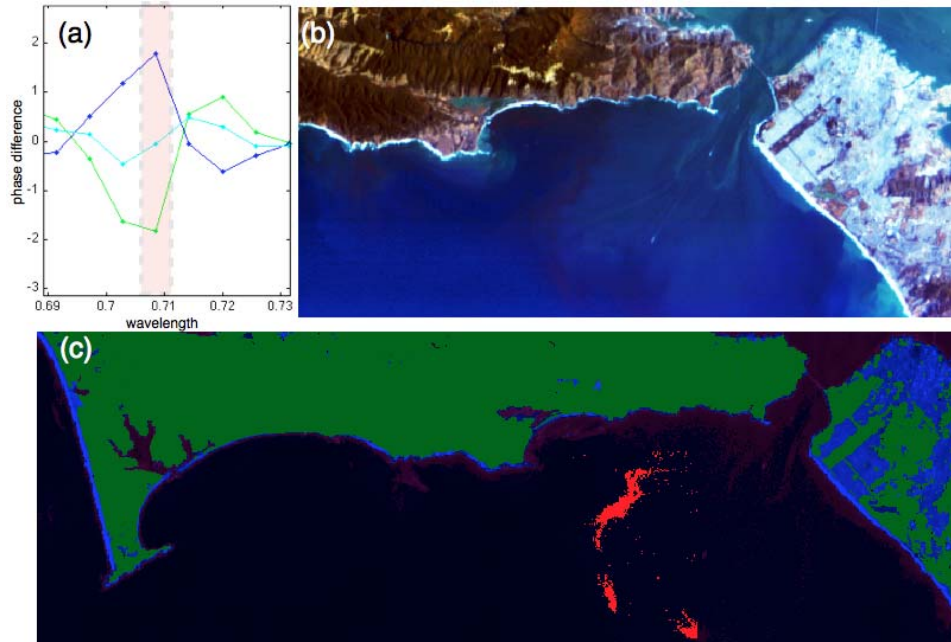


Figure 7. (a) The phase difference function for spectra at the mouth of the San Francisco Bay showing that the 709 nm HICO channel can be used to indicate chlorophyll rich water. (b) HICO image of the mouth of San Francisco Bay, 28 September 2011. (c) Indicator function for high chlorophyll levels which show a high concentration of chlorophyll at the interface of bay water and sea water apparently in response to large amounts of nutrients being exported from SFE.

4. DISCUSSION AND CONCLUSIONS

The use of derivative data, in addition to the original spectral radiances is helpful since it can highlight significant features. This observation has been used often in the past for identification of laboratory spectra, and it is possible to directly adapt laboratory identification methods, such as derivative spectroscopy, to remote sensing product estimation. Derivative spectroscopy has previously been used to identify optimal spectral channels for the design of multi-spectral instruments²¹ and to estimate coastal bottom types from aerial hyperspectral data⁴. Here we illustrate the use of methods adapted from derivative spectroscopy for product generation from HICO data. The detection of these underlying absorptive and fluorescent signatures can be sharpened by the use of derivative spectroscopy. Specifically, peaks with narrower half-widths grow more quickly with the order of the derivative. This is illustrated in Fig. 5 where we show that the derivative helps to highlight signatures sensitive to sediment in Columbia River spectra. Spectral features identified in this way can create products which are 'regionally tuned,' and built on historical data specific to a coastal area. Our method for deriving sediment and pigment products from HICO is similar to that recently described by Gitelson, et al¹⁸. They used HICO data to create a regionally tuned chlorophyll-a product for the Azov Sea. They pick the bands for the product and then optimize the choice of bands for a band-ratio algorithm based on *in situ* data. Their method is also informed by derivative analysis in their choice of the final bands for the regression. Our method differs in that we build our optimization using all the HICO wavelengths, and instead of testing for the sensitivity to specific bands, our

sensitivity is based on the principal components which are a linear combination of all the wavelengths. Specifically, the method we describe could contain details about the spectral shape - such as spectral bandwidths - which might not be utilized in the method of Gitelson and co-workers.

All of these results highlight the advantages of hyperspectral imaging. Future NASA ocean color sensors including PACE, GEO-CAPE and HypsIRI are all planned to be hyperspectral sensors with 5 nm spectral sampling or better, similar to HICO. HICO's 93 m spatial resolution is excellent for sampling the coastal ocean. However, HICO samples selected targets only, and an instrument designed to sample the entire coastal ocean should have a coarser resolution to maximize area coverage. Earlier studies^{22,23} indicated that 300 to 500 m resolution was adequate for most coastal regions when the bottom is not imaged. This was recently confirmed by Aurin, et al.²⁴ who found that a pixel size of 520 m or smaller was needed to sample large river plumes and other coastal features. Based on these results we strongly urge that the PACE sensor have a coastal mode with 500 m or better sampling. The threshold science requirements for GEO-CAPE require a 375 m pixel size at nadir which translates to approximately 500 m in U.S. coastal waters for this geostationary sensor located over the Equator. The preferred baseline requirement is 250 m which would provide approximately 300 m resolution for U.S. coastal waters. HypsIRI is primarily a land imager but will provide 60 m pixel size data valuable for coastal areas particularly when the bottom is imaged resulting in a much more spatially complex scene.

ACKNOWLEDGEMENTS

We thank the Naval Research Laboratory for the design, development and operation of HICO. We thank the Office of Naval Research for funding the development and initial operations of HICO. We thank the NASA International Space Station Program for supporting having HICO on the station and for the 2013 and ongoing operations of HICO including the science support at OSU. Our work on rivers was supported by grant N000141010448 from the Office of Naval Research. We thank Jasmine Nahorniak for help editing this manuscript.

REFERENCES

- [1] Lucke, R. L., M. Corson, N. R. McGlothlin, S. D. Butcher, D. L. Wood, D. R. Korwan, R.-R. Li, W. A. Snyder, C. O. Davis, and D. T. Chen, "The Hyperspectral Imager for the Coastal Ocean (HICO): Instrument Description and First Images," *Applied Optics*, V. 50 (11): 1501-1516 doi:10.1364/AO.50.001501 (2011).
- [2] Corson, M. and C. Davis, "The Hyperspectral Imager for the Coastal Ocean (HICO) provides a new view of the Coastal Ocean from the International Space Station," *AGU EOS*, V. 92(19): 161-162 (2011).
- [3] Gao, B-C, R.-R. Li, R. L. Lucke, C. O. Davis, R. M. Bevilacqua, D. R. Korwan, M. J. Montes, J. H. Bowles and M. R. Corson, "Vicarious calibrations of HICO data acquired from the International Space Station," *Applied Optics*, V. 51 (14): 2559-2567 (2012).
- [4] Louchard, E. M., R. P. Reid, C. F. Stephens, C. O. Davis, R. A. leathers, T. V. Downes and R. Maffione, "Derivative analysis of absorption features in hyperspectral remote sensing data of carbonate sediments," *Optics Express*, 10(26): 1573-1584 (2002).
- [5] Tuffillaro, N. B., C. O. Davis, and K. B. Jones, "Indicators of plume constituents from HICO," *Ocean Optics 2010*, 27 Sept – 1 Oct 2010, Anchorage, AK (2010).
- [6] Tuffillaro, N. B., and C. O. Davis, "Derivative spectroscopy with HICO," *Proc. Optical Remote Sensing of the Environment (ORS)*, Monterey, CA, June 25, 2012, Optical Society of America (2012).
- [7] Ortiz, J.D., "Application of Visible/near Infrared derivative spectroscopy to Arctic paleoceanography," *IOP Conf. Series: Earth and Environmental Science* 14, 012011 doi:10.1088/1755-1315/14/1/012011 (2011).
- [8] Ali, Khalid A., Donna L. Witter, and Joseph D. Ortiz. "Multivariate approach to estimate colour producing agents in Case 2 waters using first-derivative spectrophotometer data," *Geocarto International* ahead-of-print (2013): 1-26 (2013).
- [9] C. Bachmann, T. Ainsworth, and R. Fusina, "Exploiting manifold geometry in hyperspectral imagery," *IEEE Transactions on Geoscience and Remote Sensing* 43(3), 441-454 [doi:10.1109/TGRS.2004.842292] (2005).
- [10] Chen, Z., & Curran, P. J., "Derivative Reflectance Spectroscopy to Estimate Suspended Sediment Concentration", *Remote Sens. Environ.*, 40:67 (1992).

- [11] Talsky, G., [Derivative Spectrophotometry], Weihein, Verlagsgesellschaft, Weihein, Germany, (1994).
- [12] Savitzky, A., and M.J.E. Golay, "Smoothing and Differentiation of Data by Simplified Least Squares Procedures". *Analytical Chemistry* **36** (8): 1627–1639. doi:10.1021/ac60214a047 (1964).
- [13] Tuffillaro, N., "The shape of ocean color," in *Topology and Dynamics of Chaos*, Editors C. Letellier and R. Gilmore, World Scientific Publishing, pp. 251-268 (2013).
- [14] Warrick, J. A., J. J. Duda, C. S. Magirl, and C. A. Curran, "River Turbidity and Sediment Loads During Dam Removal," *AGU EOS*, V. 93(43): 425-426 (2012).
- [15] Gong, G-C, J. Chang, K.-P. Chiang, T.-M. Hsiung, C.-C. Hung, S.-W. Duan, and L. A. Codispoti, "Reduction of primary production and changing of nutrient ratio in the East China Sea: Effect of the Three Gorges Dam?" *Geophys. Res. Letters*, Vol. 33, L07610, doi:10.1029/2006GL025800 (2006).
- [16] Chen, S., G. Zhang, and S. Yang, "Temporal and spatial changes of suspended sediment concentration and resuspension in the Yangtze River estuary," *J. Geogr. Sci.*, 13, 498– 506 (2003).
- [17] Rast, M., Bezy, J. L., & Bruzzi, S., "The ESA medium resolution imaging spectrometer MERIS - a review of the instrument and its mission," *International Journal of Remote Sensing*, 20, 1681–1702 (1999).
- [18] Gitelson A. A, B-C. Gao, R-R. Li, S. Berdnikov and V. Saprygin, "Estimation of chlorophyll-a concentration in productive turbid waters using a Hyperspectral Imager for the Coastal Ocean—the Azov Sea case study," *Environ. Res. Lett.* 6 (2011) 024023, 1-6 (2011).
- [19] Hickey, B.M., et al., "River Influences on Shelf Ecosystems: Introduction and synthesis," *J. Geophys. Res.* 115:1-26, C00B17, doi:10.1029/2009JC005452 (2010).
- [20] Banas, N. S., P. MacCready, and B. M. Hickey, "The Columbia River plume as a cross-shelf exporter and along-coast barrier," *Continental Shelf Res.*, 29:292-301 (2009).
- [21] Lee, Z-P., K. Carder, R. Arnone, and M-X He, "Determination of primary spectral bands for remote sensing of aquatic environments," *Sensors* 7: 3428-3441 (2007).
- [22] Bissett, W. P., R. A. Arnone, C. O. Davis, T. D. Dickey, D. Dye, D. R. Kohler, and R. W. Gould, Jr., "From Meters to Kilometers: A look at ocean-color scales of variability, spatial coherence, and the need for fine-scale remote sensing in coastal ocean optics," *Oceanography*, 17(2): 32-43 (2004).
- [23] Davis, C.O., M. Kavanaugh, R. Letelier, W. P. Bissett and D. Kohler, "Spatial and Spectral Resolution Considerations for Imaging Coastal Waters," *Proc. SPIE* V. 6680, 66800P:1-12 (2007).
- [24] Aurin, D., A. Mannino and B. Franz, "Spatially resolving ocean color and sediment dispersion in river plumes, coastal systems, and continental shelf waters," *Remote Sensing of the Environment*, V. 137: 212-225 (2013).